

Observations of N_2O_5 and $ClNO_2$ at a polluted urban surface site in North China: High N_2O_5 uptake coefficients and low $ClNO_2$ product yields



Xinfeng Wang^a, Hao Wang^a, Likun Xue^{a,*}, Tao Wang^{a,b}, Liwei Wang^a, Rongrong Gu^a, Weihao Wang^b, Yee Jun Tham^b, Zhe Wang^b, Lingxiao Yang^a, Jianmin Chen^a, Wenxing Wang^a

^a Environment Research Institute, Shandong University, Ji'nan, Shandong, China

^b Department of Civil and Environmental Engineering, The Hong Kong Polytechnic University, Hong Kong, China

HIGHLIGHTS

- Relatively low N_2O_5 but high $ClNO_2$ were observed in a polluted urban area in China.
- N_2O_5 was lost very fast on aerosol surfaces with high uptake coefficients.
- $ClNO_2$ yields from heterogeneous N_2O_5 uptake were low despite high chloride content.

ARTICLE INFO

Article history:

Received 3 September 2016

Received in revised form

22 February 2017

Accepted 24 February 2017

Available online 27 February 2017

Keywords:

Dinitrogen pentoxide

Nitryl chloride

Uptake coefficient

Product yield

Urban China

ABSTRACT

Dinitrogen pentoxide (N_2O_5) and its heterogeneous uptake product, nitryl chloride ($ClNO_2$), play important roles in the nocturnal boundary layer chemistry. To understand the abundances and chemistry of N_2O_5 and $ClNO_2$ in the polluted urban atmosphere in North China, field measurements were conducted by deploying a chemical ionization mass spectrometer in urban Ji'nan in September 2014. The observed surface N_2O_5 concentrations were relatively low, with an average nocturnal value of 22 pptv, although the source of NO_3 was rather strong, i.e., the NO_2 and O_3 were at very high levels. The N_2O_5 concentration peaked in the early evening, which was associated with thermal power plant plumes and residual O_3 . Nocturnal N_2O_5 was lost very rapidly, mainly through heterogeneous reactions on aerosol surfaces. The estimated N_2O_5 uptake coefficient was in the range of 0.042–0.092, among the highest values obtained from ground based field measurements. The fast heterogeneous reaction of N_2O_5 on high loadings of aerosols generated relatively high levels of $ClNO_2$, with an average nocturnal concentration of 132 pptv. Despite the rich chloride content in aerosols, the $ClNO_2$ product yield was low, 0.014 and 0.082 in two nighttime cases, much lower than the calculated values from the experiment-derived parameterization. The suppressed chlorine activation in polluted urban atmospheres was possibly associated with the reduced hygroscopicity, solubility, and activity of chloride in complex ambient aerosols.

© 2017 Elsevier Ltd. All rights reserved.

1. Introduction

Dinitrogen pentoxide (N_2O_5) and nitryl chloride ($ClNO_2$) have been identified as important reactive nitrogen species in the polluted troposphere (Brown et al., 2006; Osthoff et al., 2008). N_2O_5 is produced reversibly from the nitrate radical (NO_3), which forms

via the reaction of NO_2 with O_3 and normally accumulates at nighttime. It is removed through various chemical processes, including heterogeneous uptake of N_2O_5 , photolysis of NO_3 , reactions of NO_3 with NO and volatile organic compounds (VOCs), and so on (Brown and Stutz, 2012). In the nocturnal boundary layer, the loss of N_2O_5 is to a large extent controlled by heterogeneous reactions on sub-micrometer aerosols, leading to fine nitrate formation (Chang et al., 2011). In particular, the heterogeneous reactions of N_2O_5 on chloride-containing aerosols can release $ClNO_2$, which serves as an important source of Cl atoms and consequently

* Corresponding author.

E-mail address: xuelikun@sdu.edu.cn (L. Xue).

contributes to the atmospheric oxidation capacity the next day (Tham et al., 2014; Thornton et al., 2010; Xue et al., 2015; Wang et al., 2016). Due to the significant effects of N_2O_5 and ClNO_2 on both particulate matter pollution and photochemical smog, close attention has been paid to their abundance as well as their chemistry in the past decade.

The heterogeneous removal of N_2O_5 and activation of ClNO_2 are governed by two key parameters, the N_2O_5 uptake coefficient (γ) and ClNO_2 product yield (ϕ). The uptake coefficient of N_2O_5 on aerosol surfaces varies with the aerosol composition. Acidic sulfates, chlorides, mineral substances, and liquid water in aerosols accelerate N_2O_5 uptake, whereas nitrates and organic matter exhibit a suppression effect (Bertram and Thornton, 2009; Brown et al., 2006; Morgan et al., 2015; Seisel et al., 2005). The ClNO_2 yield from N_2O_5 heterogeneous reactions strongly depends on the content of liquid water and dissolved chloride within the particles. Laboratory studies have developed a parameterization formula that fits the ClNO_2 yield as a function of chloride concentration and water content (Behnke et al., 1997; Bertram and Thornton, 2009; Roberts et al., 2009) and it is widely used in modeling studies (Sarwar et al., 2012, 2014). Nevertheless, owing to the complexity of the real atmospheric environment and the various types of aerosol, field measurements have shown large variability in γ and ϕ values with location, and significant discrepancies have been found in the two values for ambient measurements and laboratory studies (Bertram and Thornton, 2009; Bertram et al., 2009; Osthoff et al., 2008; Phillips et al., 2016; Riedel et al., 2012; Riemer et al., 2009).

The complex nocturnal chemistry of N_2O_5 and ClNO_2 in polluted urban environments is of particular importance because of the intensive anthropogenic emissions of NO_x and VOCs from traffic and industry, the high levels of secondary pollutants of sub-micrometer aerosol and O_3 , and the complicated ground surface owing to various types of land use. In the past decade, a number of field studies on N_2O_5 and ClNO_2 have been conducted in or over urban areas, downwind areas and polluted coastal sites, mainly in North America and Europe, revealing the large influence of anthropogenic activities. Elevated nocturnal concentrations of N_2O_5 (or NO_3) typically build up with high levels of O_3 and NO_2 but low levels of NO and humidity, whereas the loss and hence lifetime are dominated by heterogeneous uptake of N_2O_5 and/or homogeneous reactions of NO_3 with anthropogenic VOCs (Asaf et al., 2009, 2010; Benton et al., 2010; Brown et al., 2016; Wagner et al., 2013; Zheng et al., 2008). Tower and aircraft based measurements have shown that the concentration and chemistry of N_2O_5 across the boundary layer is strongly altitude dependent, with larger concentrations and longer lifetime at higher altitudes than those at the surface (Benton et al., 2010; Brown et al., 2007, 2009, 2013; Stutz et al., 2004, 2010). The low levels of N_2O_5 at the urban surface are generally attributed to the abundant NO from freshly emitted vehicle exhausts, especially in the cold season (Benton et al., 2010; Zheng et al., 2008). Urban plumes and power plant plumes are apt to produce high levels of N_2O_5 and the heterogeneous product ClNO_2 at higher altitude because of the high concentrations of precursors and sometimes the high ClNO_2 yield (Brown et al., 2007, 2013; Riedel et al., 2012, 2013; Zaveri et al., 2010). Recent field measurements near megacities in East Asia also revealed high or very high levels of N_2O_5 and ClNO_2 , which were attributed to the transport of urban/industrial plumes with abundant O_3 and NO_x and led to enhanced production of O_3 and RO_x radicals the following day (Brown et al., 2016; Tham et al., 2014, 2016; Wang et al., 2016). Despite the above findings, few studies have been conducted on N_2O_5 and ClNO_2 in polluted urban environments in North China, where the atmospheric characteristics and chemistry may be unique.

Ji'nan, the capital city of Shandong province, is located close to

the center of North China. It has a population of 7.0 million and 1.4 million vehicles in 2014 (Shandong Provincial Bureau of Statistics, <http://www.stats-sd.gov.cn/tjnj/nj2014/indexch.htm>). Due to the intensive emissions from industrial and other anthropogenic sources, Ji'nan and the surrounding areas have experienced severe particulate matter pollution and photochemical pollution in the past decade (Wang et al., 2014; Wen et al., 2015; Sun et al., 2016). To understand the abundances of N_2O_5 and ClNO_2 , the uptake coefficient, and the product yield in urban areas of North China, simultaneous measurements of N_2O_5 and ClNO_2 were taken in urban Ji'nan in late summer of 2014. The concentrations and characteristics of N_2O_5 and ClNO_2 were presented, and then the loss of N_2O_5 and the production of ClNO_2 were analyzed and discussed in detail, with the expectation of obtaining a comprehensive understanding of the chemistry of N_2O_5 and ClNO_2 in the polluted urban boundary layer in this region.

2. Experiments and methods

2.1. Site description

The measurement site is situated in urban Ji'nan ($36^\circ 40' \text{ N}$, $117^\circ 03' \text{ E}$) in North China. The field measurements were taken at the Urban Atmospheric Environment Observation Station (UAEOS) on the 7th floor ($\sim 22 \text{ m}$ above ground level) of a teaching building in the central campus of Shandong University (SDU) from August 31 to September 21, 2014. The UAEOS-SDU site is surrounded by dense buildings for teaching, living, and business, among which a number of trees are distributed. There are major and minor roads nearby with a large traffic flow, especially in rush hour, and the vehicles emit large amounts of NO_x into the atmosphere (mostly as NO). Some large-scale industries are located in suburban areas (see Fig. 1). To the north and northeast of the UAEOS-SDU site, there are several thermal power plants (TTP), two steel plants (SP), and one oil refinery plant (ORP). To the southwest are several cement plants (CP) and a TTP. The coal-combustion industries near the site emit smoke plumes containing abundant SO_2 and NO_x (usually dominated by NO_2).

2.2. Instruments and supporting data

N_2O_5 and ClNO_2 were simultaneously measured by iodide-chemical ionization mass spectrometry (CIMS) (THS Instruments Inc., USA), which combines ion–molecule chemistry and mass spectrometry (Kercher et al., 2009). The CIMS used in this study was the same one and had a similar setup to that in our previous studies at Mt. TMS in Hong Kong and at rural Wangdu in the North China Plain (Tham et al., 2016; Wang et al., 2016). Briefly, the sample inlet was installed $\sim 1.5 \text{ m}$ above the roof of the UAEOS-SDU site. Air samples were drawn through a 4-m PFA-Teflon tube ($1/4'' \text{ O. D.}$) at a total flow rate of $\sim 11 \text{ SLPM}$, and only 1.7 SLPM of the air flow was drawn into the CIMS for subsequent ion–molecule reactions and detection. All of the tubing and fittings were replaced daily with clean ones to avoid particle deposition and tubing loss. The abundance of N_2O_5 and ClNO_2 was quantified by the signals of $\text{I}(\text{N}_2\text{O}_5)^+$ at 235 amu and $\text{I}(\text{ClNO}_2)^+$ at 208 amu with a time resolution of 8 s . The N_2O_5 sensitivity was determined using the on-line synthetic method with standard N_2O_5 produced from reactions of NO_2 with O_3 (Bertram et al., 2009). The ClNO_2 sensitivity was determined by passing a known concentration of N_2O_5 through the NaCl slurry (Roberts et al., 2009). The background signals of the CIMS were examined periodically by forcing the sample flow through a filter packed with activated carbon and were generally low. For the detailed information on the measurement protocols and quality assurance and quality control procedures, please refer to Wang

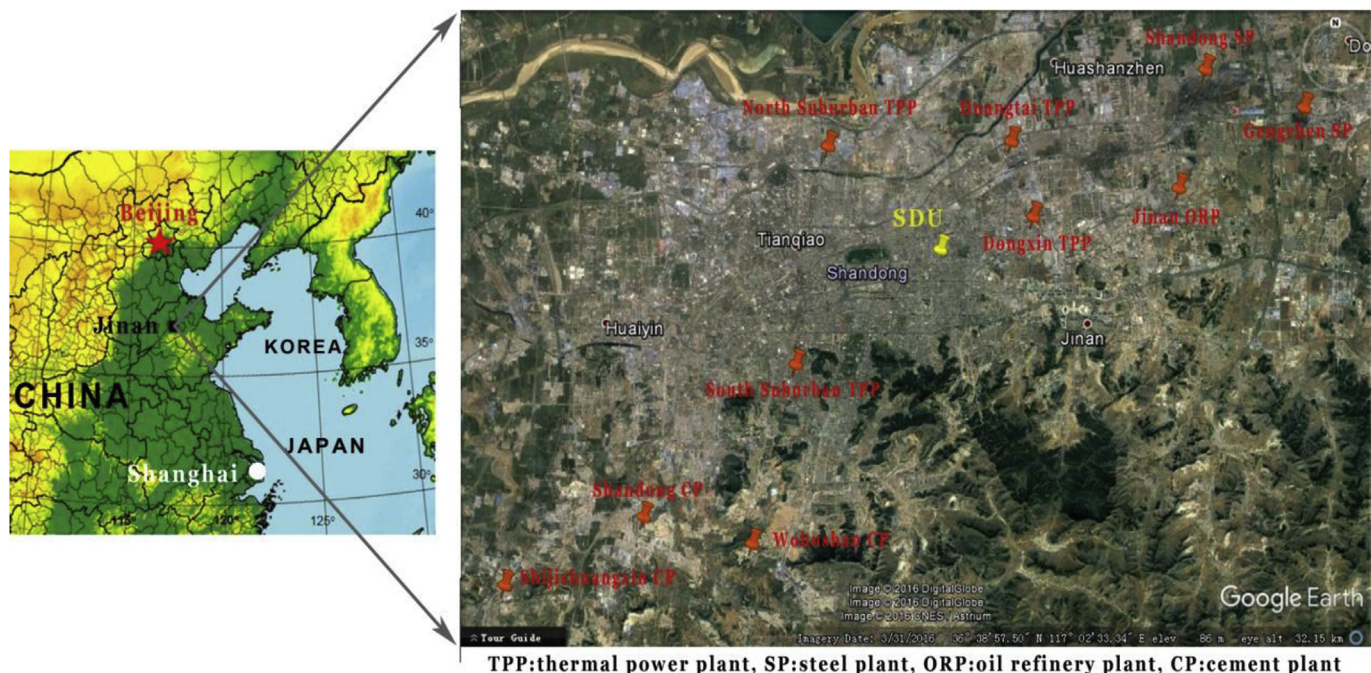


Fig. 1. Location of Ji'nan & the sampling site, where some large industries are operated.

et al. (2016) and Tham et al. (2016).

Concurrently, several other trace gases were measured. NO (nitric oxide) and NO₂ were measured with a chemiluminescence NO_x analyzer (Model 42i, Thermo Environmental Instruments (TEI), USA) coupled with a highly selective photolytic converter (BLC, Meteorologie Consult GmbH, Germany), with detection limit of 0.05 ppbv for an integration time of 5 min (Xu et al., 2013). Ozone was measured with a commercial UV photometric instrument (Model 49i, TEI, USA). SO₂ was detected by the pulsed fluorescence method (Model 43C, TEI, USA) and CO was measured by the IR radiation absorption method (Model 300E, Teledyne Advanced Pollution Instrumentation (API), USA). All of these gas analyzers were equipped with an inlet filter to prevent particles. They were calibrated every three days with zero air and mixed standard gas.

Hourly PM_{2.5} concentration data were obtained from the local air quality monitoring network (<http://58.56.98.78:8801/airdeploy.web/AirQuality/MapMain.aspx>). The PM_{2.5} at the site of Seed Co., Ltd. Shandong Province (SCL-SDP) was used in this study. This location is 1.8 km from our AEOS-SDU site and has a similar surrounding environment. The on-line hourly PM_{2.5} concentrations from the SCL-SDP site were consistent with the off-line 12-hr data at the AEOS-SDU site and thus were believed to be applicable. Aerosol surface area density (*A*) was estimated from the hourly PM_{2.5} concentration, based on the linear correlation between PM_{2.5} (measured by SHARP 5350, Thermal Scientific, USA) and *A* (measured by WPS 1000XP, MSP, USA) obtained the same season in 2013 ($R^2 = 0.75$). Note that the sizes of aerosols measured by WPS in 2013 represent particle diameters under nearly dry conditions. To take into account the hygroscopic growth of aerosols in high humidity, the aerosol surface area data used in this study were corrected with a growth factor. The growth factor was calculated by a parameterized formula expressed as a function of relative humidity (RH): $GF = a \left(b + \frac{1}{1-RH} \right)^{1/3}$ (Lewis, 2008). The values of *a* and *b* were 0.582 and 8.46 for the nighttime periods based on the field measurements over the North China Plain by Achtert et al. (2009). The estimated aerosol surface area density with

consideration of the hygroscopic growth was very high during this field campaign, in the levels of 3028–9194 $\mu\text{m}^2 \text{cm}^{-3}$, which are comparable to the measured aerosol surface area values in September 2013. The uncertainty of the aerosol surface area data used in this study was estimated to be ~30%.

Inorganic water-soluble ions in PM_{2.5} were also measured in this study. PM_{2.5} samples were collected on quartz filters using a medium-volume sampler (TH-150, Tianhong, China) every 12 h (08:00 to 20:00 local time for daytime samples and 20:00 to 08:00 for nighttime samples). PM_{2.5} filter samples were then dissolved completely in deionized water followed by ionic analysis by ion chromatography (ICs-90, Dionex, USA). An AS14A Column and an AMMS 300 Suppressor were used to detect anions including Cl⁻, NO₃⁻, and SO₄²⁻. A CS12A Column and a CSRS Ultra II Suppressor were used to detect cations including Na⁺, NH₄⁺, K⁺, Mg²⁺, and Ca²⁺.

The liquid water and dissolved ion contents in PM_{2.5} samples were calculated via an online aerosol inorganics model (AIM-IV) (Wexler and Clegg, 2002), with input data of ambient concentrations of major ions including H⁺, NH₄⁺, Na⁺, SO₄²⁻, NO₃⁻, Cl⁻, relative humidity, and temperature (*T*). The AIM model can be run on the website <http://www.uea.ac.uk/~e770/aim.html>.

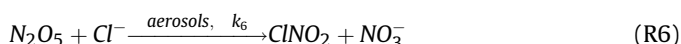
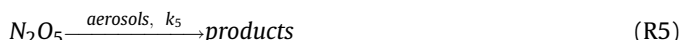
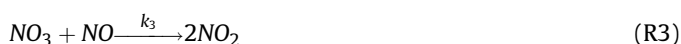
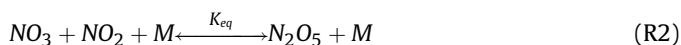
Due to lack of measurements data, the concentrations of 38 VOCs, including ethane, ethene, ethyne, propane, propene, i-butane, n-butane, 1-butene, i-butene, *trans*-2-butene, *cis*-2-butene, i-pentane, n-pentane, 1,3-butadiene, 1-pentene, isoprene, *trans*-2-pentene, *cis*-2-pentene, 3-methyl-1-butene, 2-methyl-1-butene, 2-methyl-2-butene, n-hexane, n-heptane, n-octane, n-nonane, 2,3-dimethylbutane, 2-methylpentane, 3-methylpentane, 2,4-dimethylpentane, 2,2,4-trimethylpentane, cyclopentane, cyclohexane, benzene, toluene, ethylbenzene, m-xylene, p-xylene, and o-xylene, were estimated based on other pollutant/parameter together with the correlations. Specifically, the concentrations of anthropogenic VOCs (37 VOCs except isoprene) were estimated according to the measured CO concentrations and the linear relationships between VOCs and CO concentrations from our previous field measurements at an urban site. The isoprene

concentration was estimated according to the measured temperature and the linear relationships between isoprene and ambient temperature. The sum of the estimated concentrations of 38 VOCs was in the range of 11.8–126.8 ppbv.

In addition, meteorological parameters including temperature, relative humidity, wind speed and direction were measured by a meteorological station (Huayun, China). NO₂ photolysis frequency (j_{NO_2}) was measured using a filter radiometer (Meteorologie Consult GmbH, Germany).

2.3. Chemical reactions and calculations

In the nocturnal boundary layer, NO₃ is mainly produced from the reaction of NO₂ with O₃ (R1), with the reaction rate constant k_1 as a function of the ambient temperature. It further reacts with NO₂ to reversibly form N₂O₅ (R2), with a temperature-dependent equilibrium constant of K_{eq} . The gas-phase loss of NO₃ primarily includes the reaction with NO (R3) with a temperature-dependent reaction rate constant of k_3 , and the oxidations of various VOCs (R4) with the NO₃ loss frequency k_4 as the sum of the products of each VOC concentration and the corresponding reaction rate constant. The direct loss of N₂O₅ mainly depends on the heterogeneous uptake of N₂O₅ on aerosol surfaces (R5), with the N₂O₅ loss frequency approximately as a function of the mean molecular speed, the uptake coefficient, and the aerosol surface area density. Particularly, the heterogeneous reactions of N₂O₅ on chloride-containing aerosols release ClNO₂ (R6), with the production rate coefficient k_6 as the product of the ClNO₂ yield and the heterogeneous N₂O₅ loss frequency.



Under conditions of warm weather, stable air mass, and far from fresh NO_x source, the fast source and loss processes of NO₃ and N₂O₅ as well as the rapid equilibrium between them are ready to establish a near instantaneous steady state. As a result, the NO₃ concentration can be estimated with the measured N₂O₅ concentration divided by the product of the equilibrium constant K_{eq} and the NO₂ concentration (see Eq. (1)). The loss frequencies of N₂O₅ via indirect homogeneous reactions of NO₃ with NO and VOCs and via direct heterogeneous hydrolysis of N₂O₅ on aerosol surface can be calculated according to Eq. (2), Eq. (3), and Eq. (4), respectively.

$$[NO_3] = \frac{[N_2O_5]}{K_{eq}[NO_2]} \quad (1)$$

$$L_{NO} = \frac{k_1[NO]}{K_{eq}[NO_2]} \quad (2)$$

$$L_{VOCs} = \frac{1.5 \times \sum_i (k_{VOC.a.i} [VOC.a]_i) + 3.5 \times k_{isoprene} [isoprene]}{K_{eq}[NO_2]} \quad (3)$$

$$L_{aerosol} \approx \frac{1}{4} \bar{c} \gamma A \quad (4)$$

Here, $[NO_3]$, $[N_2O_5]$, $[NO_2]$, and $[NO]$ are the concentrations of NO₃, N₂O₅, NO₂, and NO, respectively. The $[VOC.a]_i$ and $k_{VOC.a, i}$ stand for the concentration of one of the 37 anthropogenic VOCs and the corresponding reaction rate constant with NO₃, respectively. The $[isoprene]$ and $k_{isoprene}$ represent the isoprene concentration and the reaction rate constant with NO₃, respectively. The \bar{c} , γ , and A are the mean molecular speed of N₂O₅, the N₂O₅ uptake coefficient, and the aerosol surface area density, respectively. The reaction rate constants used in this study were all adopted from the IUPAC (International Union of Pure and Applied Chemistry) website (Atkinson et al., 2004, 2006). Note that to minimize the underestimation of loss of NO₃ and thus N₂O₅ through VOCs oxidation caused by the limited species of VOCs estimated in Section 2.2, the calculated NO₃ loss frequency arose from anthropogenic VOCs was enlarged by timing a factor of 1.5 and that arose from biogenic VOCs was enlarged by timing a factor of 3.5 (Yan et al., 2005).

With assumption of a balance between the direct and indirect losses of NO₃ and N₂O₅ and their production in steady state, the reciprocal of the steady-state lifetime of NO₃ can be expressed as the sum of the indirect NO₃ loss frequency through heterogeneous uptake of N₂O₅ and the direct NO₃ loss frequency k_g via gas-phase reactions with NO and VOCs (see Eq. (5)) (Brown et al., 2006; Phillips et al., 2016). Therefore, if the $(\tau_{NO_3})^{-1}$ exhibits a linear correlation with the $(K_{eq}[NO_2])$ during a selected period, the N₂O₅ uptake coefficient γ can be estimated based on the linear slope between $(\tau_{NO_3})^{-1}$ and $\frac{1}{4} \bar{c} A K_{eq} [NO_2]$.

$$\begin{aligned} (\tau_{NO_3})^{-1} &= \frac{[NO_3]}{k_1[NO_2][O_3]} = \frac{[N_2O_5]}{(k_1[NO_2][O_3])(K_{eq}[NO_2])} \\ &= k_5(K_{eq}[NO_2]) + k_g \approx \frac{1}{4} \bar{c} \gamma A (K_{eq}[NO_2]) + k_g \end{aligned} \quad (5)$$

Within a stable air mass (e.g., there are only relatively small variations in the primary and precursor species), the increase in ClNO₂ concentration mainly arises from the ClNO₂ formation via heterogeneous N₂O₅ reactions on chloride-containing aerosols. In such condition, the ClNO₂ production yield ϕ can be calculated from the production rate of ClNO₂ and the heterogeneous loss rate of N₂O₅ (see Eq. (6)).

$$\Phi = \frac{d[ClNO_2]/dt}{\frac{1}{4} \bar{c} \gamma A [N_2O_5]} \quad (6)$$

3. Observational results

3.1. Concentration levels

Time series of hourly concentrations of N₂O₅, ClNO₂, other related pollutants, and the photolysis frequency of NO₂ during the field campaign are shown in Fig. 2. Overall, N₂O₅ and ClNO₂ concentrations exhibited large variations from night to night. The average N₂O₅ and ClNO₂ mixing ratios were 17 ± 11 pptv and 94 ± 58 pptv (average \pm standard deviation). The mean nighttime N₂O₅ concentration, 22 ± 13 pptv, was significantly higher than that for daytime. The maximum hourly concentration of N₂O₅, 278 pptv,

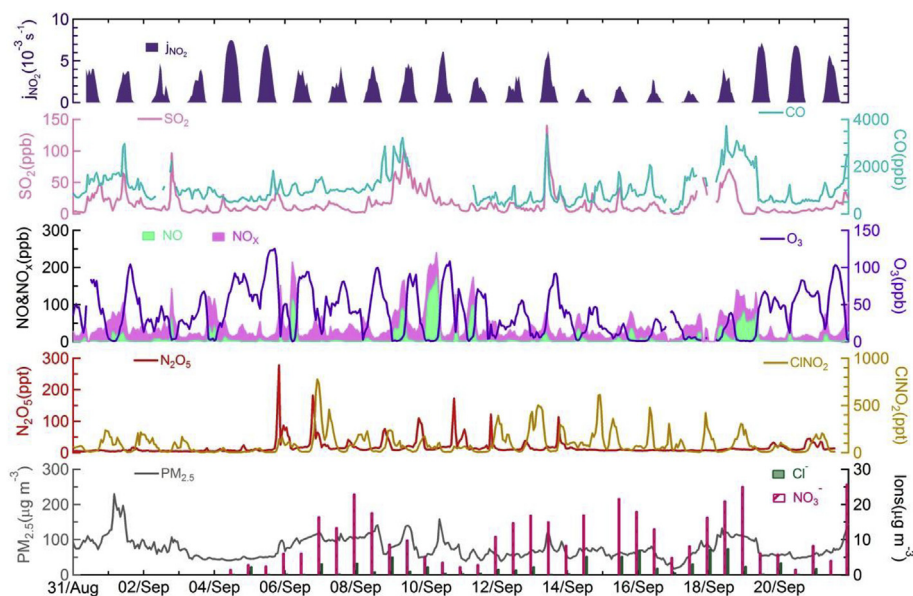


Fig. 2. Time series of hourly concentrations of N_2O_5 , $ClNO_2$, other related pollutants, and NO_2 photolysis frequency.

was recorded in the evening of September 5, with corresponding NO_2 of 74.6 ppbv and O_3 of 55 ppbv. Compared with other locations in Asia, North America, and Europe, urban Ji'nan had higher levels of precursors of NO_2 and O_3 , but lower concentrations of N_2O_5 (as shown in Table 1).

Compared to N_2O_5 , the concentration of $ClNO_2$ at ground level in urban Ji'nan was moderately high and exhibited a different variation pattern. The mean nocturnal concentration of $ClNO_2$ was 132 ± 43 pptv, and the maximum hourly mixing ratio reached 776 pptv, which appeared on the night of September 7. The concentration peaks of $ClNO_2$ appeared with a time lag of 1–3 h and lasted for a much longer period than N_2O_5 , possibly owing to its relatively long lifetime. The $ClNO_2$ -to- N_2O_5 ratios in urban Ji'nan varied from several to dozens pptv/pptv, much higher than those observed in other locations, such as the rural continental region (0.2–3) (Phillips et al., 2012) and an urban background site (0.02–2.4) (Bannan et al., 2015).

During the measurement period of 22 days, there were 10 nights on which the N_2O_5 exhibited apparent concentration peaks. To obtain a comprehensive understanding of the chemistry of N_2O_5 (and also $ClNO_2$) in urban Ji'nan, six nighttime cases (September 5, 6, 9, 12, 13, and 20) with concurrent high concentration peaks of N_2O_5 and $ClNO_2$ but without an injection of freshly emitted NO

plumes, are analyzed in detail in the following sections.

3.2. Diurnal variations

The average diurnal variations of N_2O_5 , $ClNO_2$, other trace gases, and meteorological parameters are illustrated in Fig. 3. N_2O_5 exhibited a sharp concentration peak at 20:00 with an average maximum value of 50 pptv, whereas $ClNO_2$ concentration presented a broad peak throughout the night with the average maximum value appearing at 22:00. Compared with other field studies (Brown et al., 2004; Wood et al., 2005), the N_2O_5 peak time in urban Ji'nan was relatively earlier. NO and NO_2 had two concentration peaks in the rush hours in the morning and in the early evening. SO_2 concentration exhibited one daytime peak in the morning and one nighttime peak in the early evening—almost at the same time as the N_2O_5 peak. Ozone concentration showed a maximum at 15:00 in the afternoon, with a significant trough corresponding to the big NO peak in the morning. A relatively high level of residual O_3 was still present in the early evening when the N_2O_5 peaks appeared. The average ambient temperature was moderately high, ranging from 20.3 °C to 25.6 °C. The humidity was moderate, with RH varying from 57.5% to 79.0%.

Table 1

Peak concentrations of N_2O_5 and the corresponding NO_2 and O_3 concentrations observed in Ji'nan and other locations.

Location	Type	Instrument	Height	N_2O_5 (pptv)	NO_2 (ppbv)	O_3 (ppbv)	Reference
East coast of USA	Coastal	CaRDS	Sea level	175	6	35	Brown et al., 2004
California, USA	Coastal	LIF	290 m asl	200	13	14	Wood et al., 2005
Tokyo, Japan	Urban	LIF	130 m asl	800	70	3	Matsumoto et al., 2005
Mexico City, Mexico	Urban	ID-CIMS	30 m agl	60	42	22	Zheng et al., 2008
London, England	Urban	LED-BBCEAS	160 m agl	450	14	14	Benton et al., 2010
Taunus, Germany	Mountain	OA-CRDS	825 m asl	550	2	50	Crowley et al., 2010
Southern Spain	Coastal	CaRDS	5–10 m agl	400	10	25	Crowley et al., 2011
Fairbanks, USA	High latitude	CRDS	400 asl	80	10	20	Huff et al., 2011
Shanghai, China	Urban	DOAS	20 m agl	3250	22.5	50	Wang et al., 2013
Mt. TMS, HK	Mountain	CIMS	975 m asl	8000	11	60	Wang et al., 2016
Northwestern Europe	Airborne	BBCEAS	—	670	6.2	42	Morgan et al., 2015
Ji'nan, China	Urban	CIMS	22 m agl	278	74.6	55	This study

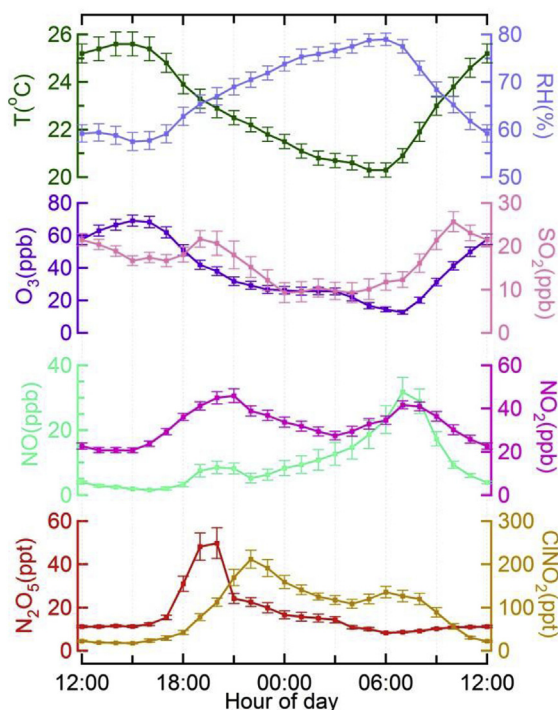


Fig. 3. Diurnal variations of N_2O_5 , $ClNO_2$, other related pollutants and parameters for the whole campaign. Error bar represents standard error.

3.3. Evening N_2O_5 peaks

To understand the origins of the evening N_2O_5 concentration peaks, we examined the 5-min data of N_2O_5 , $ClNO_2$, NO_x , SO_2 , O_3 , aerosol surface area density, relative humidity, temperature, and wind speed and direction in the six nighttime cases (shown in Fig. 4). The maximum 5-min concentration of N_2O_5 (430 pptv) appeared at 20:45 on September 5, with concurrent 60.9 ppbv NO_2 and 61 ppbv O_3 . In the early evening of September 5, the wind mainly originated from the north and the SO_2 mixing ratio stayed very high, with an average value of 57.9 ppbv, indicating that the polluted air mass was a coal combustion plume from thermal power plants in the north of Ji'nan (see Fig. 1). Once the wind changed to the south at 21:00, both NO and NO_2 concentrations increased rapidly followed by a gradual decrease in SO_2 , suggesting that the air mass changed from a thermal power plant plume to a vehicle exhaust-dominated or mixed urban plume. As a result, the O_3 mixing ratio exhibited a sharp reduction and the N_2O_5 concentration dropped to a very low level. Similarly, the nighttime cases on September 6, 9, and 13 also exhibited high N_2O_5 concentration peaks (above 100 pptv) in the thermal power plant plumes (SO_2 exceeding 10 ppbv) and a sharp drop after the air masses changed (characterized by changes in wind direction and concentrations of NO_x and O_3). Unlike the former four cases, the SO_2 concentrations were relatively low (mostly below 10 ppbv) in the evenings of September 12 and 20, indicating weak influence from coal combustion plumes. At this time, the NO_2 concentrations were moderate, at ~ 20 ppbv, which generated relatively low levels of N_2O_5 with a peak concentration of ~ 40 pptv. In summary, the elevated evening concentration peaks of N_2O_5 observed in urban Ji'nan were associated with northerly thermal power plant plumes in which high concentrations of NO_2 and O_3 were present.

4. Discussion

4.1. Estimation of N_2O_5 uptake coefficient

To understand the loss of N_2O_5 and the heterogeneous uptake coefficient on aerosol surfaces, $(\tau_{NO_3})^{-1}$ were calculated according to Eq. (5), and scatter plots and linear regressions were made between $(\tau_{NO_3})^{-1}$ and $\frac{1}{4}\bar{c}AK_{eq}[NO_2]$ for selected periods in the six nighttime cases (see Fig. 5; 19:00–21:00 at the night of September 5, 19:00–06:00 at the night of September 6, 18:00–23:00 at the night of September 9, 18:00–23:00 at the night of September 12, 18:00–23:00 at the night of September 13, and 18:00–03:30 at the night of September 20). These periods were chosen with relatively high and variable levels of N_2O_5 and NO_2 , but very low concentration of NO which indicates little influence from the fresh emission source of NO_x . During each period, the ambient temperature was relatively high, averagely in the range of 21.0–27.3 °C. The wind speed was generally low (< 1.0 m s^{-1}) and the wind was often from the same direction, suggesting relatively stable air masses. The air mass was confirmed to be in steady state by running a box model of MCM v3.3 with consideration of both homogeneous and heterogeneous processes associated with NO_3 and N_2O_5 . The observed relevant pollutant concentrations and meteorological parameters as well as the calculated uptake coefficient (see below) were taken as the inputs. The outputted N_2O_5 concentration changed within a small range and appeared to be stabilizing within two minutes.

Based on the linear slopes of the scatter plots shown in Fig. 5 (correlation coefficients all above 0.82), the estimated N_2O_5 uptake coefficient γ were listed in Table 2, ranging from 0.042 to 0.092. As shown, the γ values tended to increase with the rising humidity. At the nights of September 5 and 9, the average RH was below 50% and the γ values were 0.042 and 0.061. At the nights of September 6, 12, 13, and 20, the RH rose to 57.2%–71.6% and the γ values increased to 0.068–0.092. Compared with other ground based field studies in West United states, Southwest Germany, and South China (Bertram et al., 2009; Brown et al., 2016; Phillips et al., 2016; Riedel et al., 2012; Wagner et al., 2013), the observed N_2O_5 uptake coefficients in this study are among the highest.

The estimated uptake coefficients were further used to calculate the loss frequencies of N_2O_5 via heterogeneous hydrolysis (according to Eq. (4)) during the six nighttime cases which were then compared with the loss frequencies of the indirect removal pathways (calculated based on Eq. (2) and Eq. (3)). The direct N_2O_5 loss frequency via heterogeneous uptake for the selected periods was in the range of 0.012–0.030 s^{-1} . The heterogeneous loss frequency of N_2O_5 on aerosol surfaces contributed three fourths (76.6%, on average) of the total N_2O_5 loss, mainly due to the high aerosol loading in this region. The fast heterogeneous loss rate of N_2O_5 on aerosol surfaces caused rapid production of particulate nitrate and gas-phase $ClNO_2$ (e.g., an increase of 10.3 $\mu g m^{-3}$ in fine nitrate concentration and a sharp peak of 972 pptv $ClNO_2$ on the night of September 6, see Fig. 2). In consideration of the high heterogeneous uptake coefficient of N_2O_5 on mineral substances (Karagulian et al., 2006; Seisel et al., 2005) and the large surface area of urban ground (Baergen et al., 2015), the urban ground surface might also contributed to the heterogeneous loss of N_2O_5 . It has been reported that the ocean surface contributed a large fraction to the loss of N_2O_5 in the coastal marine boundary layer (Kim et al., 2014) and that the snow surface played an import role in the rapid loss of N_2O_5 at high latitudes (Apodaca et al., 2008). The indirect loss frequency of N_2O_5 caused by VOCs oxidation by NO_3 varied from 0.002 to 0.009 s^{-1} , with an average contribution of 16.3%. The loss

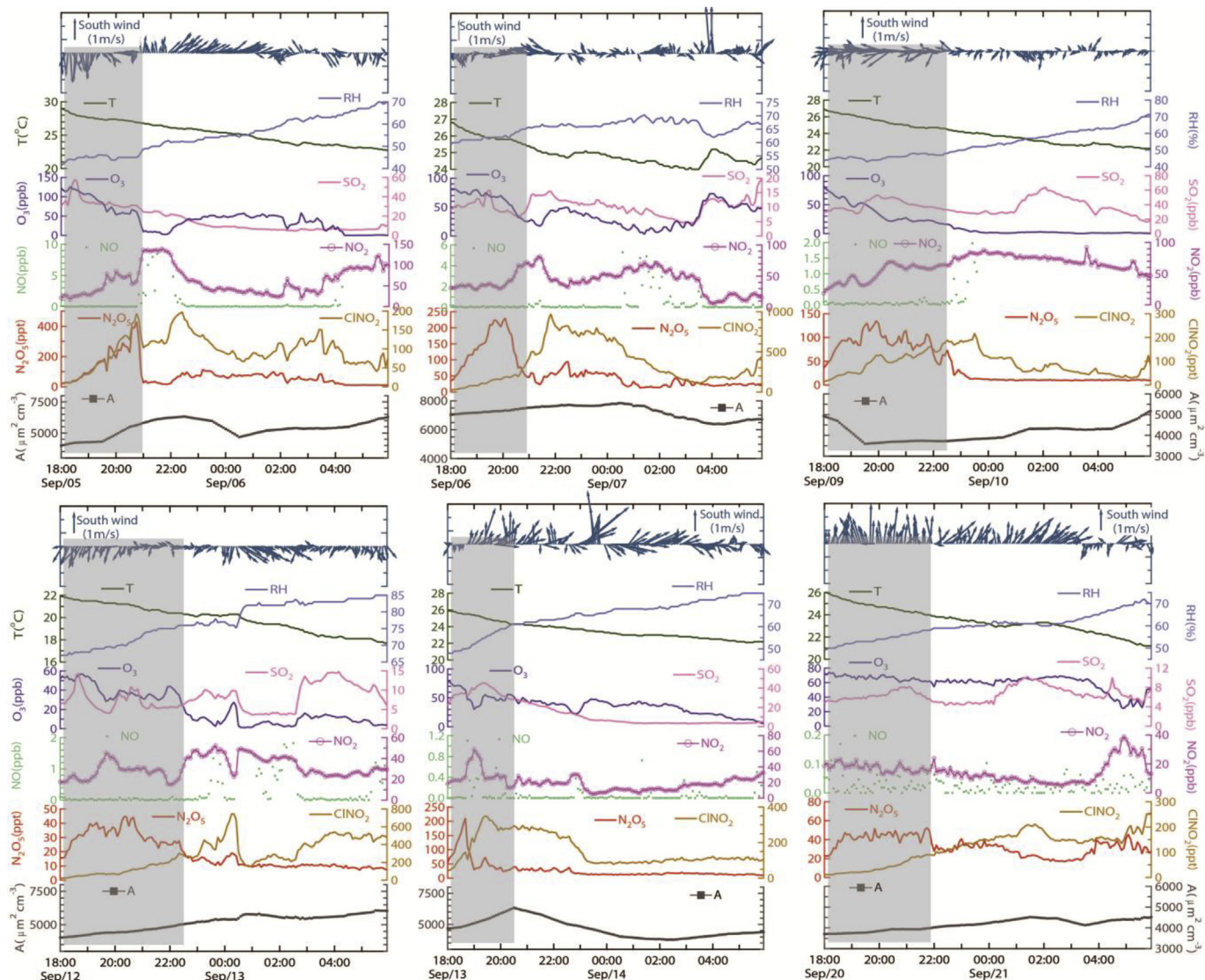


Fig. 4. Time series of gases, aerosol surface area density, and meteorological parameters for six evening N_2O_5 peaks on September 5, 6, 9, 12, 13 and 20.

frequency through gas-phase reaction of NO_3 with NO was between 0.0006 and $0.004 s^{-1}$, contributing 7.1% to the total N_2O_5 loss. For each period, the sum of the calculated indirect N_2O_5 loss frequencies were generally consistent with the k_g divided by $K_{eq}[NO_2]$, further indicating the applicability of the inverse lifetime analysis in estimation of N_2O_5 uptake coefficient. Overall, the removal of N_2O_5 in urban Ji'nan was dominated by the fast heterogeneous reactions which led to a relatively low abundance of N_2O_5 at the ground level.

4.2. Derivation of $ClONO_2$ product yield

To obtain a comprehensive understanding of the relatively high levels of $ClONO_2$ at ground level in urban Ji'nan, we selected two proper periods at the nights of September 6 and 20 to calculate the production yield of $ClONO_2$. As shown in Fig. 6, during the two selected periods of 20:35–21:50 on September 6 and 20:00–1:30 on September 20, the wind directions were almost the same, from the southeast or south. The humidity was relatively stable, with average RH of 65.7% and 58.8% . The N_2O_5 concentration and the aerosol surface area density also exhibited small changes, with

average values of 50 and 36 pptv, and 7545 and $4124 \mu m^2 cm^{-3}$, respectively. During these two periods, the $ClONO_2$ concentration exhibited nearly linear increases, generating production rates of 8.40 and 0.55 ppt min^{-1} . According to Eq. (3) and the estimated N_2O_5 uptake coefficient, the derived production yield in the two cases was 0.082 and 0.014 , substantially lower than those observed in other locations including the southeast coastline of the United States (0.1 – 0.65) (Osthoff et al., 2008) and continental Colorado (0.07 – 0.36) (Thornton et al., 2010).

In addition, we compared the observed $ClONO_2$ yield with the parameterized calculation with the data of liquid water content and aqueous chloride content. The concentration of chloride in fine particles in urban Ji'nan was rather high (2.8 and $4.4 \mu g m^{-3}$ in the two nighttime cases), which resulted in a high chloride content in aerosol liquid water (2.1 and $3.7 mol L^{-1}$). As shown in Table 3, the $ClONO_2$ yield observed in urban Ji'nan increased with rising relative humidity and chloride content. Surprisingly, the observed $ClONO_2$ yields were much lower than those calculated via the parameterized formula by Roberts et al. (2009). The lower values of observed $ClONO_2$ yield indicate that the yields used in the modeling studies might be significantly overestimated, which should be considered.

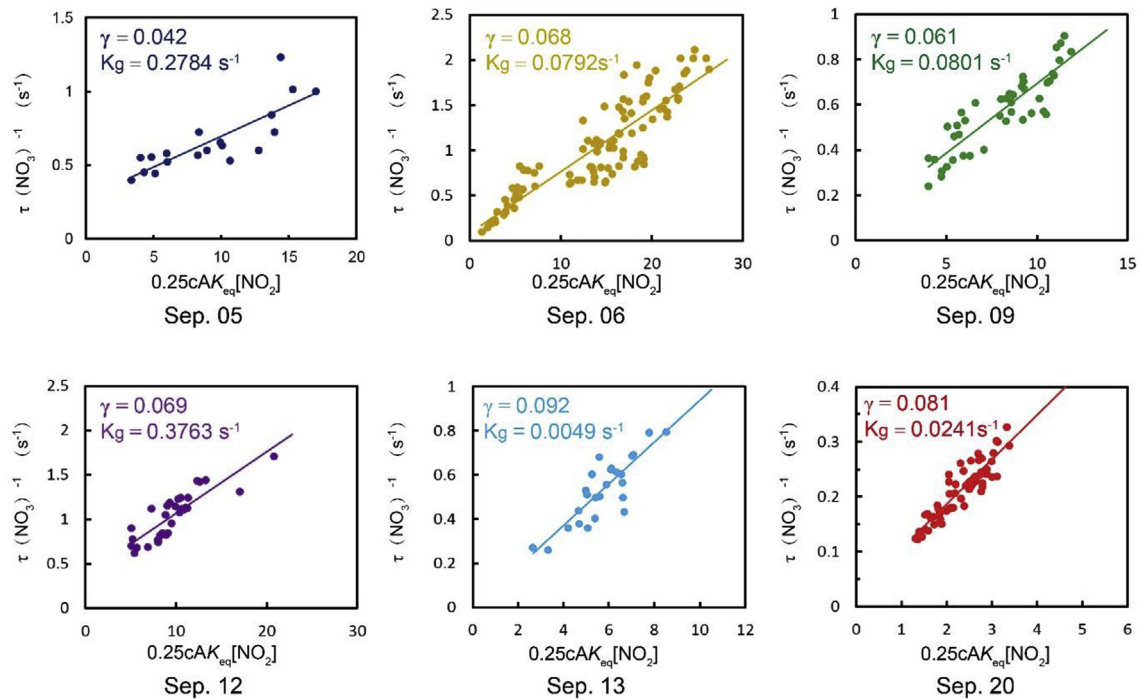


Fig. 5. N_2O_5 uptake coefficients derived from scatter plots of $\tau(\text{NO}_3)^{-1}$ versus $0.25cA_{\text{eq}} \times [\text{NO}_2]$ for six selected periods on the nights of September 5, 6, 9, 12, 13 and 20.

Table 2
Estimated uptake coefficient of N_2O_5 and related parameters for selected periods in six nighttime cases.

Nighttime case	T (°C)	RH (%)	N_2O_5 (pptv)	γ	k_g (s^{-1})	Correlation coefficient
Sep. 5	27.3	43.4	213	0.042	0.2784	0.82
Sep. 6	24.9	66.0	57	0.068	0.0792	0.88
Sep. 9	25.4	46.2	83	0.061	0.0801	0.88
Sep. 12	21.0	71.6	29	0.069	0.3763	0.85
Sep. 13	24.6	58.5	48	0.092	0.0049	0.85
Sep. 20	23.9	57.9	33	0.081	0.0241	0.91

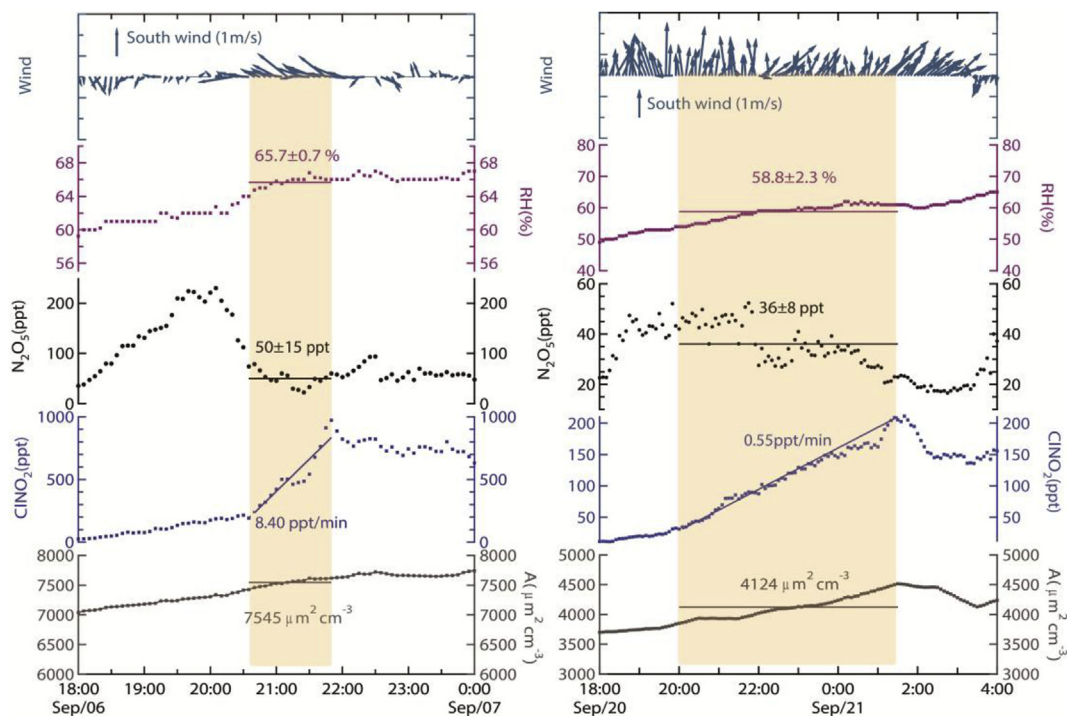


Fig. 6. Time series of wind, relative humidity, N_2O_5 and ClNO_2 concentrations, and aerosol surface area density, for two nighttime cases on September 6 and 20, showing nearly linear increase of ClNO_2 .

Table 3Observation and parameterization based ClNO₂ yield and related parameters for selected periods in two nighttime cases.

Nighttime case	RH (%)	ClNO ₂ (pptv)	Cl ⁻ (air) (μg m ⁻³)	Cl ⁻ (aq) (mol L ⁻¹)	Observed φ	Parameterized φ*
Sep. 6	65.7	508	4.4	2.1	0.082	0.945
Sep. 20	58.8	115	2.8	3.7	0.014	0.968

* Estimated ClNO₂ yields via the parameterized formula by Roberts et al. (2009).

The difference in ClNO₂ yield between field measurements and laboratory studies was thought to be related to the altered dissolution of chloride in real atmospheric aerosols. This suggests possible suppressed the hygroscopicity, solubility, and reactivity of chloride in complex ambient aerosols due to internal mixing with or coated by water insoluble substances (Laskin et al., 2012; Li et al., 2016; Semeniuk et al., 2007; Thornton and Abbatt, 2005; Ryder et al., 2014). Further studies are required to clarify the causes.

5. Summary and conclusions

Field measurements of N₂O₅ and ClNO₂ were conducted in a polluted atmosphere at an urban site in Ji'nan in North China from August 31 to September 21, 2014. During the measurement period, the precursors of N₂O₅ (i.e., NO₂ and O₃) were abundant; however, the N₂O₅ concentration at ground level was relatively low with an average nocturnal value of 22 pptv. The N₂O₅ concentration peaked mostly in the evening, which was associated with coal combustion plumes emitted from thermal power plants to the north of the city. Fast heterogeneous uptake was the main cause of the low levels of N₂O₅ observed in urban Ji'nan. The estimated heterogeneous uptake coefficient of N₂O₅ from our field study was rather high, in the range of 0.042–0.092, increasing positively with the ambient humidity. Furthermore, the fast heterogeneous reactions of N₂O₅ on chloride aerosols yielded moderately high levels of ClNO₂ with average nocturnal concentration of 132 pptv. The ClNO₂ yield was relatively low, 0.014 and 0.082 in two nighttime cases, increasing remarkably with rising humidity and chloride content. Notably, the observed ClNO₂ yield was significantly lower than those calculated from the laboratory parameterization formula, suggesting possible suppressed hygroscopicity, solubility, and activity of chloride in complex ambient aerosols.

Acknowledgments

The authors would like to thank the anonymous reviewers for their helpful comments and suggestions. We would also like to thank Xue Yang for her help on the MCM tests. This work was supported by the National Natural Science Foundation of China (Nos. 91544213, 41275123, 21407094) and the Natural Science Foundation of Shandong Province (No. ZR2014BQ031).

References

- Achtert, P., Birmili, W., Nowak, A., Wehner, B., Wiedensohler, A., Takegawa, N., Kondo, Y., Miyazaki, Y., Hu, M., Zhu, T., 2009. Hygroscopic growth of tropospheric particle number size distributions over the North China Plain. *J. Geophys. Res.* 114.
- Apodaca, R.L., Huff, D.M., Simpson, W.R., 2008. The role of ice in N₂O₅ heterogeneous hydrolysis at high latitudes. *Atmos. Chem. Phys.* 8, 7451–7463.
- Asaf, D., Pedersen, D., Matveev, V., Peleg, M., Kern, C., Zingler, J., Platt, U., Luria, M., 2009. Long-term measurements of NO₃ radical at a Semiarid urban site: 1. Extreme concentration events and their oxidation capacity. *Environ. Sci. Technol.* 43, 9117–9123.
- Asaf, D., Tas, E., Pedersen, D., Peleg, M., Luria, M., 2010. Long-term measurements of NO₃ radical at a Semiarid urban site: 2. Seasonal trends and loss mechanisms. *Environ. Sci. Technol.* 44, 5901–5907.
- Atkinson, R., Baulch, D., Cox, R., Crowley, J., Hampson, R., Hynes, R., Jenkin, M., Rossi, M., Troe, J., 2004. Evaluated kinetic and photochemical data for atmospheric chemistry: volume I-gas phase reactions of O_x, HO_x, NO_x and SO_x species. *Atmos. Chem. Phys.* 4, 1461–1738.
- Atkinson, R., Baulch, D., Cox, R., Crowley, J., Hampson, R., Hynes, R., Jenkin, M., Rossi, M., Troe, J., 2006. Evaluated kinetic and photochemical data for atmospheric chemistry: volume II-gas phase reactions of organic species. *Atmos. Chem. Phys.* 6, 3625–4055.
- Baergen, A.M., Styler, S., van Pinxteren, D., Müller, K., Herrmann, H., Donaldson, D.J., 2015. Chemistry of urban grime: inorganic ion composition of grime vs. particles in Leipzig, Germany. *Environ. Sci. Technol.* 49, 12688–12696.
- Bannan, T.J., Booth, A.M., Bacak, A., Muller, J., Leather, K.E., Le Breton, M., Jones, B., Young, D., Coe, H., Allan, J., 2015. The first UK measurements of nitryl chloride using a chemical ionization mass spectrometer in central London in the summer of 2012, and an investigation of the role of Cl atom oxidation. *J. Geophys. Res.* 120, 5638–5657.
- Behnke, W., George, C., Scheer, V., Zetzsch, C., 1997. Production and decay of ClNO₂ from the reaction of gaseous N₂O₅ with NaCl solution: bulk and aerosol experiments. *J. Geophys. Res.* 102, 3795–3804.
- Benton, A.K., Langridge, J.M., Ball, S.M., Bloss, W.J., Dall'Osto, M., Nemitz, E., Harrison, R.M., Jones, R.L., 2010. Night-time chemistry above London: measurements of NO₃ and N₂O₅ from the BT tower. *Atmos. Chem. Phys.* 10, 9781–9795.
- Bertram, T.H., Thornton, J.A., 2009. Toward a general parameterization of N₂O₅ reactivity on aqueous particles: the competing effects of particle liquid water, nitrate and chloride. *Atmos. Chem. Phys.* 9, 8351–8363.
- Bertram, T., Thornton, J., Riedel, T., Middlebrook, A., Bahreini, R., Bates, T., Quinn, P., Coffman, D., 2009. Direct observations of N₂O₅ reactivity on ambient aerosol particles. *Geophys. Res. Lett.* 36, L19803.
- Brown, S., Dibb, J., Stark, H., Aldener, M., Vozella, M., Whitlow, S., Williams, E., Lerner, B., Jakoubek, R., Middlebrook, A., 2004. Nighttime removal of NO_x in the summer marine boundary layer. *Geophys. Res. Lett.* 31, L07108.
- Brown, S., Ryerson, T., Wollny, A., Brock, C., Peltier, R., Sullivan, A., Weber, R., Dube, W., Trainer, M., Meagher, J., 2006. Variability in nocturnal nitrogen oxide processing and its role in regional air quality. *Science* 311, 67.
- Brown, S., Dubé, W., Osthoff, H., Stutz, J., Ryerson, T., Wollny, A., Brock, C., Warneke, C., de Gouw, J., Atlas, E., 2007. Vertical profiles in NO₃ and N₂O₅ measured from an aircraft: results from the NOAA P-3 and surface platforms during the New England air quality study 2004. *J. Geophys. Res.* 112, D22304.
- Brown, S.S., Dubé, W.P., Fuchs, H., Ryerson, T.B., Wollny, A.G., Brock, C.A., Bahreini, R., Middlebrook, A.M., Neuman, J.A., Atlas, E., Roberts, J.M., Osthoff, H.D., Trainer, M., Fehsenfeld, F.C., Ravishankara, A.R., 2009. Reactive uptake coefficients for N₂O₅ determined from aircraft measurements during the Second Texas Air Quality Study: comparison to current model parameterizations. *J. Geophys. Res.* 114, D00F10.
- Brown, S.S., Stutz, J., 2012. Nighttime radical observations and chemistry. *Chem. Soc. Rev.* 41, 6405–6447.
- Brown, S.S., Thornton, J.A., Keene, W.C., Pszenny, A.A.P., Sive, B.C., Dubé, W.P., Wagner, N.L., Young, C.J., Riedel, T.P., Roberts, J.M., VandenBoer, T.C., Bahreini, R., Öztürk, F., Middlebrook, A.M., Kim, S., Hübler, G., Wolfe, D.E., 2013. Nitrogen, Aerosol Composition, and Halogens on a Tall Tower (NACHITT): overview of a wintertime air chemistry field study in the front range urban corridor of Colorado. *J. Geophys. Res.* 118, 8067–8085.
- Brown, S.S., Dubé, W.P., Tham, Y.J., Zha, Q., Xue, L., Poon, S., Wang, Z., Blake, D.R., Tsui, W., Parrish, D.D., Wang, T., 2016. Nighttime chemistry at a high altitude site above Hong Kong. *J. Geophys. Res.* 121, 2457–2475.
- Chang, W.L., Bhavsar, P.V., Brown, S.S., Riemer, N., Stutz, J., Dabdub, D., 2011. Heterogeneous atmospheric chemistry, ambient measurements, and model calculations of N₂O₅: a review. *Aerosol Sci. Tech.* 45, 665–695.
- Crowley, J.N., Schuster, G., Pouvesle, N., Parchatka, U., Fischer, H., Bonn, B., Bingemer, H., Lelieveld, J., 2010. Nocturnal nitrogen oxides at a rural mountain-site in south-western Germany. *Atmos. Chem. Phys.* 10, 2795–2812.
- Crowley, J.N., Thieser, J., Tang, M.J., Schuster, G., Bozem, H., Beygi, Z.H., Fischer, H., Diesch, J.M., Drewnick, F., Borrmann, S., Song, W., Yassaa, N., Williams, J., Pöhler, D., Platt, U., Lelieveld, J., 2011. Variable lifetimes and loss mechanisms for NO₃ and N₂O₅ during the DOMINO campaign: contrasts between marine, urban and continental air. *Atmos. Chem. Phys.* 11, 10853–10870.
- Huff, D.M., Joyce, P.L., Fochesatto, G.J., Simpson, W.R., 2011. Deposition of dinitrogen pentoxide, N₂O₅, to the snowpack at high latitudes. *Atmos. Chem. Phys.* 11, 4929–4938.
- Karagulian, F., Santschi, C., Rossi, M.J., 2006. The heterogeneous chemical kinetics of N₂O₅ on CaCO₃ and other atmospheric mineral dust surrogates. *Atmos. Chem. Phys.* 6, 1373–1388.
- Kercher, J., Riedel, T., Thornton, J., 2009. Chlorine activation by N₂O₅: simultaneous, in situ detection of ClNO₂ and N₂O₅ by chemical ionization mass spectrometry.

- Atmos. Meas. Tech. 2, 193–204.
- Kim, M.J., Farmer, D.K., Bertram, T.H., 2014. A controlling role for the air–sea interface in the chemical processing of reactive nitrogen in the coastal marine boundary layer. *Proc. Natl. Acad. Sci.* 111, 3943–3948.
- Laskin, A., Moffet, R.C., Gilles, M.K., Fast, J.D., Zaveri, R.A., Wang, B., Nigge, P., Shutthanandan, J., 2012. Tropospheric chemistry of internally mixed sea salt and organic particles: surprising reactivity of NaCl with weak organic acids. *J. Geophys. Res.* 117, D15302.
- Lewis, E.R., 2008. An examination of Köhler theory resulting in an accurate expression for the equilibrium radius ratio of a hygroscopic aerosol particle valid up to and including relative humidity 100%. *J. Geophys. Res.* 113.
- Li, W., Shao, L., Zhang, D., Ro, C.-U., Hu, M., Bi, X., Geng, H., Matsuki, A., Niu, H., Chen, J., 2016. A review of single aerosol particle studies in the atmosphere of East Asia: morphology, mixing state, source, and heterogeneous reactions. *J. Clean. Prod.* 112 (Part 2), 1330–1349.
- Matsumoto, J., Imai, H., Kosugi, N., Kajii, Y., 2005. In situ measurement of N₂O₅ in the urban atmosphere by thermal decomposition/laser-induced fluorescence technique. *Atmos. Environ.* 39, 6802–6811.
- Morgan, W.T., Ouyang, B., Allan, J.D., Aruffo, E., Di Carlo, P., Kennedy, O.J., Lowe, D., Flynn, M.J., Rosenberg, P.D., Williams, P.I., Jones, R., McFiggans, G.B., Coe, H., 2015. Influence of aerosol chemical composition on N₂O₅ uptake: airborne regional measurements in northwestern Europe. *Atmos. Chem. Phys.* 15, 973–990.
- Osthoff, H.D., Roberts, J.M., Ravishankara, A.R., Williams, E.J., Lerner, B.M., Sommariva, R., Bates, T.S., Coffman, D., Quinn, P.K., Dibb, J.E., Stark, H., Burkholder, J.B., Talukdar, R.K., Meagher, J., Fehsenfeld, F.C., Brown, S.S., 2008. High levels of nitryl chloride in the polluted subtropical marine boundary layer. *Nat. Geosci.* 1, 324–328.
- Phillips, G.J., Tang, M.J., Thieser, J., Brickwedde, B., Schuster, G., Bohn, B., Lelieveld, J., Crowley, J.N., 2012. Significant concentrations of nitryl chloride observed in rural continental Europe associated with the influence of sea salt chloride and anthropogenic emissions. *Geophys. Res. Lett.* 39, L10811.
- Phillips, G.J., Thieser, J., Tang, M., Sobanski, N., Schuster, G., Fachinger, J., Drewnick, F., Borrmann, S., Bingemer, H., Lelieveld, J., Crowley, J.N., 2016. Estimating N₂O₅ uptake coefficients using ambient measurements of NO₃, N₂O₅, ClNO₂ and particle-phase nitrate. *Atmos. Chem. Phys.* 16, 13231–13249.
- Riedel, T.P., Bertram, T.H., Ryder, O.S., Liu, S., Day, D.A., Russell, L.M., Gaston, C.J., Prather, K.A., Thornton, J.A., 2012. Direct N₂O₅ reactivity measurements at a polluted coastal site. *Atmos. Chem. Phys.* 12, 2959–2968.
- Riedel, T.P., Wagner, N.L., Dubé, W.P., Middlebrook, A.M., Young, C.J., Öztürk, F., Bahreini, R., VandenBoer, T.C., Wolfe, D.E., Williams, E.J., Roberts, J.M., Brown, S.S., Thornton, J.A., 2013. Chlorine activation within urban or power plant plumes: vertically resolved ClNO₂ and Cl₂ measurements from a tall tower in a polluted continental setting. *J. Geophys. Res.* 118, 8702–8715.
- Riemer, N., Vogel, H., Vogel, B., Anttila, T., Kiendler-Scharr, A., Mentel, T., 2009. Relative importance of organic coatings for the heterogeneous hydrolysis of N₂O₅ during summer in Europe. *J. Geophys. Res.* 114, D17307.
- Roberts, J.M., Osthoff, H.D., Brown, S.S., Ravishankara, A., Coffman, D., Quinn, P., Bates, T., 2009. Laboratory studies of products of N₂O₅ uptake on Cl containing substrates. *Geophys. Res. Lett.* 36, L20808.
- Ryder, O.S., Ault, A.P., Cahill, J.F., Guasco, T.L., Riedel, T.P., Cuadra-Rodríguez, L.A., Gaston, C.J., Fitzgerald, E., Lee, C., Prather, K.A., Bertram, T.H., 2014. On the role of particle inorganic mixing state in the reactive uptake of N₂O₅ to ambient aerosol particles. *Environ. Sci. Technol.* 48, 1618–1627.
- Sarwar, G., Simon, H., Bhave, P., Yarwood, G., 2012. Examining the impact of heterogeneous nitryl chloride production on air quality across the United States. *Atmos. Chem. Phys.* 12, 6455–6473.
- Sarwar, G., Simon, H., Xing, J., Mathur, R., 2014. Importance of tropospheric ClNO₂ chemistry across the northern hemisphere. *Geophys. Res. Lett.* 41, 4050–4058.
- Seisel, S., Börensén, C., Vogt, R., Zellner, R., 2005. Kinetics and mechanism of the uptake of N₂O₅ on mineral dust at 298 K. *Atmos. Chem. Phys.* 5, 3423–3432.
- Semeniuk, T.A., Wise, M.E., Martin, S.T., Russell, L.M., Buseck, P.R., 2007. Hygroscopic behavior of aerosol particles from biomass fires using environmental transmission electron microscopy. *J. Atmos. Chem.* 56, 259–273.
- Stutz, J., Alicke, B., Ackermann, R., Geyer, A., White, A., Williams, E., 2004. Vertical profiles of NO₃, N₂O₅, O₃, and NO_x in the nocturnal boundary layer: 1. Observations during the Texas Air Quality Study 2000. *J. Geophys. Res.* 109, D12306.
- Stutz, J., Wong, K.W., Lawrence, L., Ziemba, L., Flynn, J.H., Rappenglück, B., Lefer, B., 2010. Nocturnal NO₃ radical chemistry in Houston, TX. *Atmos. Environ.* 44, 4099–4106.
- Sun, L., Xue, L.K., Wang, T., Gao, J., Ding, A.J., Cooper, O.W., Lin, M.Y., Xu, P.J., Wang, Z., Wang, X.F., Wen, L., Zhu, Y.H., Chen, T.S., Yang, L.X., Wang, Y., Chen, J.M., Wang, W.X., 2016. Significant increase of summertime ozone at mount. Tai in central Eastern China. *Atmos. Chem. Phys.* 16, 10637–10650.
- Tham, Y., Yan, C., Xue, L., Zha, Q., Wang, X., Wang, T., 2014. Presence of high nitryl chloride in Asian coastal environment and its impact on atmospheric photochemistry. *Chin. Sci. Bull.* 59, 356–359.
- Tham, Y.J., Wang, Z., Li, Q., Yun, H., Wang, W., Wang, X., Xue, L., Lu, K., Ma, N., Bohn, B., Li, X., Kecorius, S., Größ, J., Shao, M., Wiedensohler, A., Zhang, Y., Wang, T., 2016. Significant concentrations of nitryl chloride sustained in the morning: investigations of the causes and impacts on ozone production in a polluted region of northern China. *Atmos. Chem. Phys. Discuss.* 2016, 1–34.
- Thornton, J., Abbatt, J., 2005. N₂O₅ reaction on submicron sea salt aerosol: kinetics, products, and the effect of surface active organics. *J. Phys. Chem. A* 109, 10004–10012.
- Thornton, J., Kercher, J., Riedel, T., Wagner, N., Cozic, J., Holloway, J., Dubé, W., Wolfe, G., Quinn, P., Middlebrook, A., 2010. A large atomic chlorine source inferred from mid-continental reactive nitrogen chemistry. *Nature* 464, 271–274.
- Wagner, N.L., Riedel, T.P., Young, C.J., Bahreini, R., Brock, C.A., Dubé, W.P., Kim, S., Middlebrook, A.M., Öztürk, F., Roberts, J.M., Russo, R., Sive, B., Swarthout, R., Thornton, J.A., VandenBoer, T.C., Zhou, Y., Brown, S.S., 2013. N₂O₅ uptake coefficients and nocturnal NO₂ removal rates determined from ambient wintertime measurements. *J. Geophys. Res.* 118, 9331–9350.
- Wang, S., Shi, C., Zhou, B., Zhao, H., Wang, Z., Yang, S., Chen, L., 2013. Observation of NO₃ radicals over Shanghai, China. *Atmos. Environ.* 70, 401–409.
- Wang, T., Tham, Y.J., Xue, L., Li, Q., Zha, Q., Wang, Z., Poon, S.C.N., Dubé, W.P., Blake, D.R., Louie, P.K.K., Luk, C.W.Y., Tsui, W., Brown, S.S., 2016. Observations of nitryl chloride and modeling its source and effect on ozone in the planetary boundary layer of southern China. *J. Geophys. Res.* 121, 2476–2489.
- Wang, X., Chen, J., Sun, J., Li, W., Yang, L., Wen, L., Wang, W., Wang, X., Collett Jr., J.L., Shi, Y., Zhang, Q., Hu, J., Yao, L., Zhu, Y., Sui, X., Sun, X., Mellouki, A., 2014. Severe haze episodes and seriously polluted fog water in Ji'nan, China. *Sci. Total. Environ.* 493, 133–137.
- Wen, L., Chen, J., Yang, L., Wang, X., Caihong, X., Sui, X., Yao, L., Zhu, Y., Zhang, J., Zhu, T., Wang, W., 2015. Enhanced formation of fine particulate nitrate at a rural site on the North China Plain in summer: the important roles of ammonia and ozone. *Atmos. Environ.* 101, 294–302.
- Wexler, A.S., Clegg, S.L., 2002. Atmospheric aerosol models for systems including the ions H⁺, NH₄⁺, Na⁺, SO₄²⁻, NO₃⁻, Cl⁻, Br⁻, and H₂O. *J. Geophys. Res.* 107, 4207.
- Wood, E.C., Bertram, T.H., Wooldridge, P.J., Cohen, R.C., 2005. Measurements of N₂O₅, NO₂, and O₃ east of the San Francisco Bay. *Atmos. Chem. Phys.* 5, 483–491.
- Xu, Z., Wang, T., Xue, L.K., Louie, P.K.K., Luk, C.W.Y., Gao, J., Wang, S.L., Chai, F.H., Wang, W.X., 2013. Evaluating the uncertainties of thermal catalytic conversion in measuring atmospheric nitrogen dioxide at four differently polluted sites in China. *Atmos. Environ.* 76, 221–226.
- Xue, L.K., Saunders, S.M., Wang, T., Gao, R., Wang, X.F., Zhang, Q.Z., Wang, W.X., 2015. Development of a chlorine chemistry module for the master chemical mechanism. *Geosci. Model Dev.* 8, 3151–3162.
- Yan, Y., Wang, Z., Bai, Y., Xie, S., Shao, M., 2005. Establishment of vegetation VOC emission inventory in China. *China Environ. Sci.* 25, 110–114 (in Chinese).
- Zaveri, R.A., Berkowitz, C.M., Brechtel, F.J., Gilles, M.K., Hubbe, J.M., Jayne, J.T., Kleinman, L.L., Laskin, A., Madronich, S., Onasch, T.B., Pekour, M.S., Springston, S.R., Thornton, J.A., Tivanski, A.V., Worsnop, D.R., 2010. Nighttime chemical evolution of aerosol and trace gases in a power plant plume: implications for secondary organic nitrate and organosulfate aerosol formation, NO₃ radical chemistry, and N₂O₅ heterogeneous hydrolysis. *J. Geophys. Res.* 115, D12304.
- Zheng, J., Zhang, R., Fortner, E.C., Volkamer, R.M., Molina, L., Aiken, A.C., Jimenez, J.L., Gaeggeler, K., Dommen, J., Dusanter, S., Stevens, P.S., Tie, X., 2008. Measurements of HNO₃ and N₂O₅ using ion drift-chemical ionization mass spectrometry during the MILAGRO/MCMA-2006 campaign. *Atmos. Chem. Phys.* 8, 6823–6838.